Surface-Induced Dissociation of Protein Complex Ions in a Modified Electrostatic Linear Ion Trap

Ian J. Carrick, Joshua T. Johnson and Scott A. McLuckey*

Department of Chemistry

Purdue University

West Lafayette, IN, 47907-2084, USA

Running title: SID of protein complexes in an ELIT

*Address correspondence to:
Dr. Scott A. McLuckey
560 Oval Drive
Department of Chemistry
Purdue University
West Lafayette, IN 47907-2084, USA
Phone: (765) 494-5270
Fax: (765) 494-0239
E-mail: mcluckey@purdue.edu

Abstract

The electrostatic linear ion trap (ELIT) is a device that can provide mass analysis via frequency measurement, followed by Fourier transformation from the frequency domain to the time domain, or via time measurement in a multi-reflection time-of-flight measurement. ELIT devices have been demonstrated to be capable of relatively high mass measurement resolution as well as high-resolution ion isolation capabilities. We have been exploring the possibility of developing the ELIT geometry as a stand-alone high-performance tandem mass spectrometer for native mass spectrometry (MS) studies. In this context, it is desirable to use an activation method capable of dissociating the high-mass complexes encountered in native MS. To this end, we describe the implementation of surface-induced dissociation (SID) in an ELIT and describe initial results for protein complexes generated under native conditions in which ion isolation, fragmentation, and product ion mass analysis all occur within the ELIT.

1. Introduction

The electrostatic linear ion trap (ELIT) is a mass analyzer formed by two oppositely-facing ion-mirrors. Ions are injected into the ELIT at high energy (e.g., ~1980 eV/z in the instrument used here), after which trapping can be achieved by raising the entrance lens of the first ion-mirror to a potential above the ion's energy-to-charge ratio, or by using an in-trap potential lift to lower the ions energy below the trapping threshold[1,2,3,4]. Stable oscillations in the ELIT occur when Einzel lensing in each ion mirror focuses ions at the center of the device, with overlapping focal points[5]. By tuning the mirror-electrode potentials, energy focusing and minimization of space-charge induced incoherence is achieved[6,7,8]. Mass analysis can be performed in Fourier-transform (FT) or in closed-path multiple-reflection time-of-flight (MR-TOF) modes[9,10,11]. In MR-TOF mode, resolution increases more quickly with oscillation time than in FT-mode before reaching a maximum, though a tradeoff between unambiguous mass range and resolution occurs due to ion lapping ('race track effect'). In FT mode, no such tradeoff occurs, though resolution increases linearly with time and thus requires longer acquisition times to match MR-TOF resolution[12]. As with the Orbitrap™[13], ion frequency in the ELIT is proportional to $\frac{1}{\sqrt{\mathrm{m/z}}}$, and thus in FT mode, resolution decreases as $\sqrt{\mathrm{m/z}}$ increases. Relative to FT-ICR, where resolution is proportional to $\frac{1}{\mathrm{m/z}}$, this offers a potential advantage at the high *m/z* ratios often encountered in native mass spectrometry[14]. The ELIT, therefore, is a relatively simple geometry device that is readily fabricated and can offer many of the advantages of FT-mass spectrometry MS) and MR-TOF MS.

MS is growing in importance as a tool in structural biology, offering complementary information to techniques such as cryo-electron microscopy and X-ray crystallography[15]. Using nano-electrospray ionization (nESI)[16], soft-ionization of proteins and protein complexes is possible, enabling ion transfer into the gas phase without significantly compromising protein-protein interfaces. Use of volatile salts, such as ammonium acetate, enables electrospray of proteins from native-like solutions, which approximate biological ionic strengths and preserve native-like protein conformations[17]. Operating under such ionization conditions is often referred to as 'native MS'. Beyond measurement of protein mass and protein complex stoichiometry, native MS techniques have been developed for elucidation of structural information. Hydrogen-deuterium exchange and cross-linking, for example, can be used to infer secondary and tertiary structural information[18,19,20].

The utility of native MS is enhanced via tandem MS. Several dissociation techniques have been demonstrated in the top-down dissociation of large complexes, each with specific advantages. In collision-induced dissociation (CID), ions undergo energetic collisions with a collision gas, thereby increasing the internal energy distribution of the ions in a step-wise fashion. Because the energy gained each collision is low and the increase in energy is relatively slow, CID

favors the lowest energy fragmentation pathways, which can involve structural rearrangement[21]. For large protein complexes, a common observation upon CID is the formation of complementary highly charged monomer and a relatively low charge N-1 mer ions, which has been attributed to unfolding of the monomer prior to ejection[22]. For this reason, CID is restricted mainly to stoichiometry measurements, and top-down sequencing purposes in native MS. Ultraviolet photodissociation has proven to be useful for monomer ejection and backbone cleavages in top-down native MS.[23] Electron capture dissociation (ECD) has also been used for backbone cleavages and top-down sequencing, with some potential for structural elucidation due to a preference for cleavages of flexible regions.[24,25,26] Surface induced dissociation (SID) has also shown potential for structural elucidation in top-down native MS. In SID, ions collide with a solid surface with a controlled energy. Unlike CID, this energy is deposited rapidly and can allow for dissociation to better compete with slow structural rearrangements, such as monomer unfolding. Symmetric charge distribution between protein subunits following SID is commonly observed, with collisional cross section measurements following SID showing preservation of subunit conformation[27,28]. Additionally, the fragmentation pathways observed in SID have been shown to be 'biologically accurate', where protein-protein interfaces are cleaved in the order of their relative strengths[29,30].

We have been developing a relatively small ELIT as either the mass analyzer in a tandem mass spectrometer instrument[31,32,33] or as a device to execute all phases of a tandem mass spectrometry experiment (i.e., mass selection[34,35,36], ion activation/dissociation, and product ion mass analysis). Given the desirability to maintain low pressure in the ELIT to avoid deleterious effects of collisions on resolution, collision-induced dissociation (CID) within the ELIT is not an attractive dissociation method. To access collision-based chemistries (e.g., CID, ion-molecule reactions, and ion-ion reactions), it is better advised to use the QLIT as the reaction vessel. If the high-resolution ion isolation capabilities of the ELIT are to be used, transfer to an external device for activation/dissociation at relatively high pressure is required, which can entail significant ion losses in the transfer process. The methods that are most attractive for inducing fragmentation within or near the ELIT are photodissociation[37] and SID. We described SID experiments in an ELIT[38] with a series of tetraalkylphosphonium salts, with the largest at *m/z* 339. In this work, we demonstrate tandem mass spectrometry experiments using SID of ions of relevance to native MS. The experiments use the ELIT for ion isolation, activation/dissociation, and capture and mass analysis of the fragment ions. We note that the ELIT geometry is also commonly used as the mass analyzer for high-performance charge-detection mass spectrometry (CDMS)[30,39]. In CDMS, direct measurement of charge, and *m/z* allows for mass measurement, reducing heterogeneity from charge state distribution and allowing for assigning masses to megadalton-sized biomolecular complexes. While the work described herein involves conventional ensemble measurements (i.e., many ions can be present for a given measurement), the ability to perform SID in the ELIT may also prove to be relevant to CDMS analysis (i.e., CDMS/MS of protein complexes using SID in the ELIT).

2. Methods

2.1 Materials

Aldolase, creatine phosphokinase, hemoglobin, and triose phosphate isomerase (TIM) were purchased from Sigma-Aldrich (St. Louis, MO). Optima LC/MS grade was purchased from Fisher Scientific (Pittsburgh, PA). 50 µM (monomer) solutions of each protein were made, in 150 mM ammonium acetate.

2.2 Mass spectrometry

SID experiments were conducted on a home-built ELIT mass spectrometer, which has been described in detail[4]. Ions were generated in the positive mode by nESI using a pulled glass capillary and platinum electrode for electrical contact. Ions were transmitted through an interface region held at 0.90 Torr, before passing into a chamber at 5 x 10^{-5} Torr. Ions passed through a linear quadrupole ion guide into a DC turning quadrupole, after which they were trapped in a quadrupole linear ion trap (QLIT) containing electrodes designed to generate a linear DC gradient in the axial direction. This set of electrodes constitutes what is referred to as "linear acceleration" (LINAC), which provides control over ion motion in the axial dimension[40,41]. The rod offset of the QLIT was then ramped to 1990 V, while the LINAC electrodes were ramped to 700 V, causing ions to bunch towards the ELIT side of the QLIT. Using an ultrafast high solid-state switch (HTS 31-03-GSM, Behlke Electronics GMBH, Kronberg, Germany), the exit lens of this QLIT was pulsed to 1500 V to inject ions into the ELIT. The entrance lens of the ELIT was similarly pulsed up from 1600 V to a trapping potential of 2300 V after a delay during which ions enter the ELIT. All voltage pulse timings were precisely controlled using a pulse/delay generator (model 575, Berkeley Nucleonics, San Rafael, CA). Apodization of FT peaks was performed by applying a Hanning window to time-domain signal for all spectra shown. Mass spectra were generated by using an enhanced Fourier transform (eFT) algorithm[42,43] to generate frequency-domain spectra, which were then converted to *m/z* using a calibrated frequency to *m/z* relation.

2.3 Isolation and SID

Ion isolations were performed by switching the potential of the entrance or exit lens of the ELIT to a potential below the trapping threshold such that unwanted ions were selectively removed (mirror-switching), as has been described previously in more detail[44]. An initial crude isolation can be performed by delaying the pulse of the ELIT exit lens from a low potential to the trapping potential, such that low *m/z* ions with higher velocity strike the SID surface instead of being reflected. An upper *m/z* limit is similarly established by reducing the delay of the entrance plate switching up to a trapping potential such that higher *m/z* ions cannot traverse the distance between the QLIT and ELIT in time to be trapped. Further selective removal of unwanted ion packets may be required due to the limited resolution afforded by this "first lap" isolation and is accomplished by gating either exit or entrance lens of the ELIT briefly to a potential below the threshold for trapping. The delay of these pulses relative to injection of ions determines the degree of spatial separation that occurs in the ELIT, with a delay of half the beat period of two ion packets representing the maximal possible separation. In practice, several mirror switching pulses can be used to narrow the isolated mass range to the extent required for the application.

The ELIT was modified for SID by mounting a polished gold surface inside the aperture of the exit lens, in electrical contact with the lens (Pine Research Instrumentation, Durham, NC). The potential of the exit lens and SID surface was controlled by a solid-state switch (HTS 31-03-GSM, Behlke Electronics GMBH, Kronberg, Germany). The low potential side of this switch was connected to the output of an identical switch, such that the SID surface could be switched between a trapping potential, a low potential to impart collision energy, and an intermediate potential used to lift SID products back to injection energy. The transient times used for post-SID analysis were limited to under 10 ms due to the amount of signal available after SID before decay to undetectable levels, resulting in lower resolution SID spectra.

3. Results and Discussion:

3.1 Triose phosphate isomerase

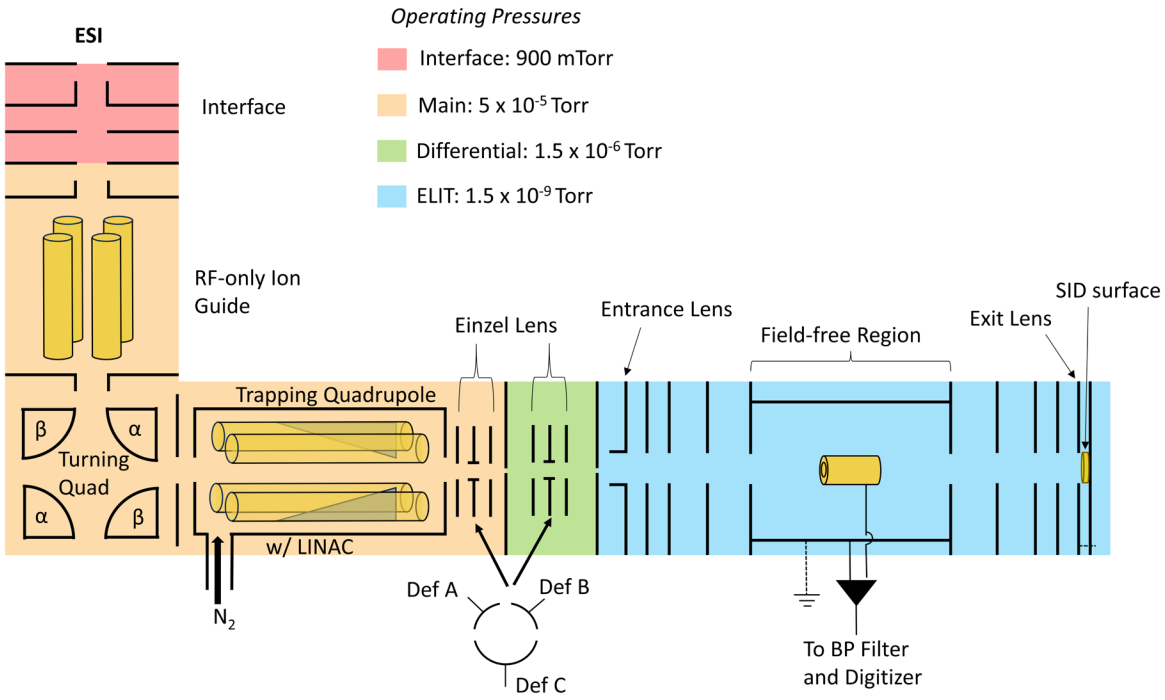

Figure 1: A schematic of the ELIT, modified with a gold surface for SID positioned directly behind the aperture of the exit lens.

Triose phosphate isomerase (TIM) is a 26.6 kDa protein primarily found in the cytosol as a dimer (53.2 kDa). The positive mode MS1 spectrum of TIM yields a dimer ion charge state distribution of 13^+ to 16^+ (Figure 2a). Prior to SID, isolation of the precursor 14^+ charge state of triose phosphate isomerase was performed using mirror-switching isolation within the ELIT (Figure 2b). An initial crude isolation was accomplished by changing the delay of the entrance and exit plates. By reducing the time delay between ejection from the QLIT and the ELIT entrance plate pulsing to a trapping potential, unwanted high *m/z* ions do not reach the ELIT in time to be

admitted. Similarly, unwanted low *m/z* ions are allowed to pass through the ELIT and strike the SID surface by delaying the pulse of the exit plate to a trapping potential. This process was effective at preventing the 16^+ charge state from being trapped. To remove neighboring charge states, the entrance plate was pulsed below trapping potential for 20 µs, a duration less than the ~33 µs lap time of the 14^+ charge state. A delay of this gate was chosen such that the 13^+ and 15^+ charge state were overlapping in time and space, while the 14^+ charge state was maximally separated spatially in the ELIT from the 13^+ and 14^+ ions. The entrance plate was then pulsed down to allow these neighboring charge states to exit the ELIT. After isolation, the exit plate was pulsed to the SID potential of 1860 V before the 14^+ charge state of TIM reached the exit plate, allowing the ion packet to collide with the SID surface (Figure 2c). Multiple charge states of the TIM monomer are observed following SID. The monomer charge state distribution is centered around the 6^+ and 7^+ charge states, showing symmetric charge partitioning as typically observed in SID[45].

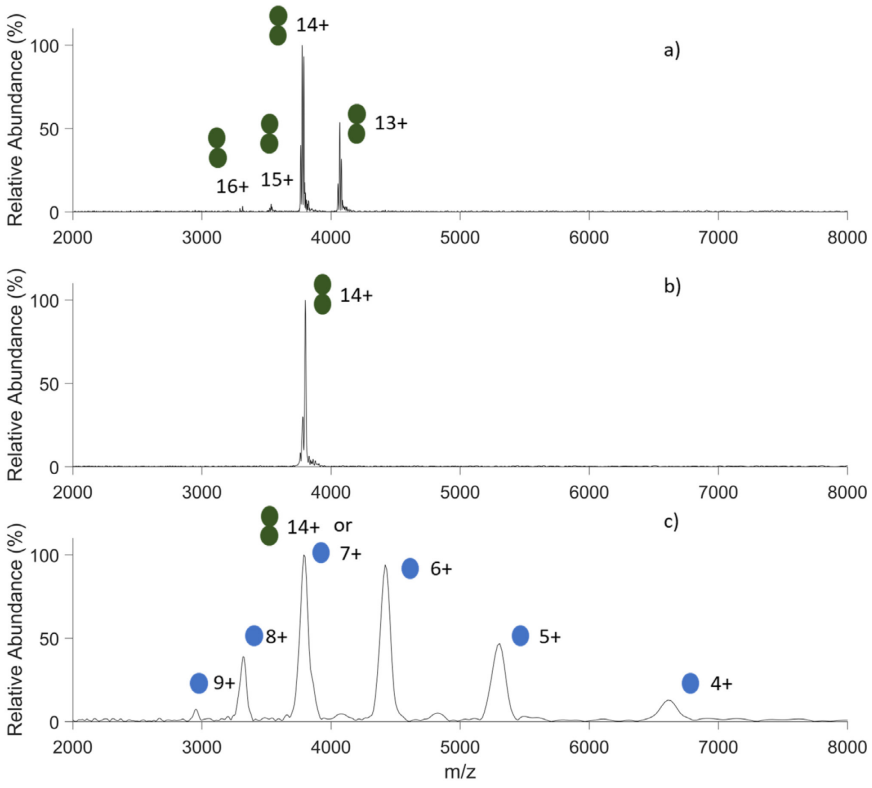

Figure 2: a) nESI mass spectrum of TIM, 30ms transient**.** b) Mirror-switching isolation of the 14^+ charge state, 50 ms transient. c) SID spectrum at 1680 eV collision energy, 5 ms transient.

The laboratory collision energy, CE, of SID can be estimated as:

$$CE = KE_{max} - zeV_{SID} \quad (1)$$

where KE_{max} is the kinetic energy in the grounded field-free region (≈1980 eV x z) and V_{SID} is the potential applied to the SID surface. The approximate timing of the precursor ion packet colliding with the surface can be empirically determined by varying the timing of the exit lens gate.

3.2 Post-SID lift

The potential of the SID surface must be reduced to result in an energetic collision. However, conditions for capture of the SID product ions are not expected to be optimal using a static reduced SID potential. For example, if all of the collision energy is lost upon SID (e.g., via transfer of all excess kinetic energy to the surface, vibrational excitation of the ion, etc.) a static SID potential would result in a much lower product ion kinetic energy. Various studies have shown low (<20%) kinetic energy retention for SID products (i.e., the ion/surface collisions are highly inelastic)[46,47,48,49]. For this reason, a second voltage pulse on the SID surface was used, which switched from the SID potential to 1980 V, the quadrupole rod offset potential used for ion injection. If this lift occurs immediately following a completely inelastic collision, the product ions would re-enter the ELIT and reach the same maximum kinetic energy-to-charge ratio as the precursor ion prior to the SID step. In practice, if products are formed with some recoil from the initial collision energy, a delay between the lift pulse and the initial pulse of the ELIT exit lens/SID surface to the SID potential is required to maximize SID product capture efficiency. Figure 3 shows post-SID spectra of TIM^{14+} collected at various delay times.

The potential at a position between the SID surface and adjacent focusing lens of the ELIT will be between the SID surface potential and the potential of this lens. Because this adjacent lens is held constant at 1600V, if ions have left the SID surface when the lift occurs, the potential lift provided at this position will be a fraction of the full potential lift at the SID surface. Figure 3 (right side) shows a schematic of the effect ion position between the SID surface and adjacent lens on the magnitude of the effected potential lift. By delaying this potential lift relative to the SID collision, SID products will have moved towards the adjacent lens when the lift occurs and thus the effective potential lift is reduced. This provides a mechanism by which tuning for average axial kinetic energy retention of SID products can be accomplished. In Figure 3, the optimal lift time for all TIM^{14+} SID products observed is the lowest lift time used (1 μs), indicating low kinetic energy retention.

Assuming a linear potential gradient between the SID surface and the adjacent lens, and that axial kinetic energy retained after the SID collision is partitioned into fragment ions by mass, the optimal delay time for the potential lift would depend on the kinetic energy retained and *m/z* of the fragment ion. Specifically,

$$T_{lift} - T_{collision} = \frac{\sqrt{\frac{2K}{M}}}{E*c*e} *(\sqrt{C^2 + C*E} - C)* m/z \quad (2)$$

where K is the retained axial kinetic energy before partitioning by mass, C is a constant equal to the rate of lift potential decrease with increasing distance from the SID surface, E is the electric

field between the SID surface and adjacent lens before the lift occurs, and M is the mass of the precursor. (See SI for a derivation of Equation 2.) SID products outside of the *m/z* range tuned for in the lift delay will therefore not be lifted to the correct energy to charge ratio for optimal trapping. Because SID usually forms products within a narrow *m/z* range due to even charge partitioning, and because these collisions are mostly inelastic, however, *m/z* dependence on the lift delay was not observed and is expected to be negligible.

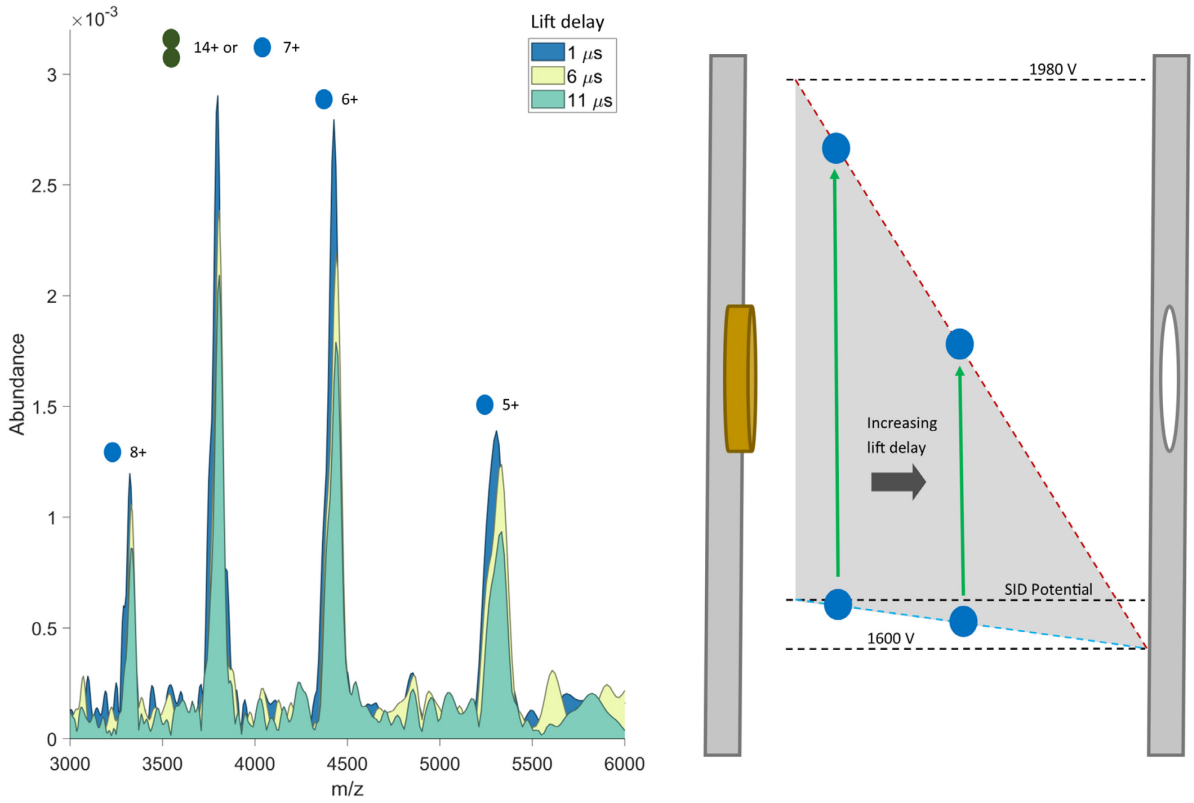

Figure 3: Overlaid spectra of TIM SID products, with varying delay of the SID lift pulse. A maximum in SID product trapping is seen at 1 µs, with further delays reducing the product intensity. Schematic: Representation of the electric potential difference from the exit lens/SID surface (left) to the adjacent lens of the ELIT. The dotted blue line represents the potential difference before the lift, while the dotted red line represents the potential difference following the lift. The lift moves an ion from the blue to the red potential line, with the magnitude of the lift dependent on the ion position, as represented by the green arrows.

3.2. Energy-resolved SID

Figure 4a shows the nESI mass spectrum of the 10^+-12^+ charge states of Hemoglobin A dimer selected via the tuned timing of the delays associated with raising the gates on the entrance and exit plates, respectively. Further isolation of the 11^+ charge state was done using a

subsequent pulse of the entrance plate, timed such that the 10+ and 12+ were overlapping while the 11+ was near maximal separation (see Figure 4b). Figure 4c provides the SID spectrum, which shows both the apo α and β monomer subunits, as well as free heme group at *m/z* 616.

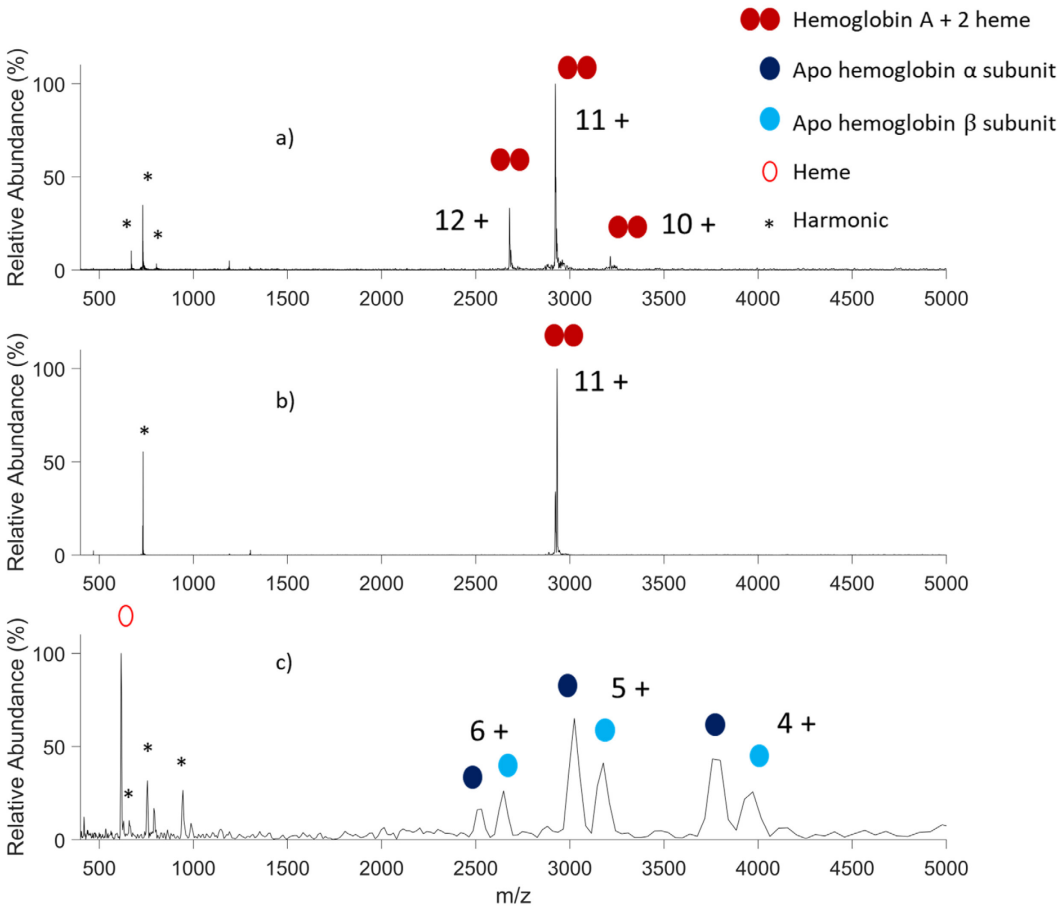

Figure 4: a) MS1 spectrum of hemoglobin, 50ms transient**.** b) Mirror-switching isolation of the 11+ charge state, 50 ms transient. c) SID spectrum at 1320 eV collision energy, 4 ms transient.

The SID collision energy can be controlled by changing the SID potential. Figure 5 shows hemoglobin A SID spectra at varying collision energies. An appearance energy of about 880 eV was found for the monomer subunits. Above 1650 eV, the monomer subunits no longer appear in the SID spectra. Likely, higher energy collisions result in access to more fragmentation channels such as internal cleavages, which divide signal to below the limit of detection. Free heme is observed to increase in intensity until 2090 eV. The ability to control SID collision energy could enable future energy-resolved SID experiments.

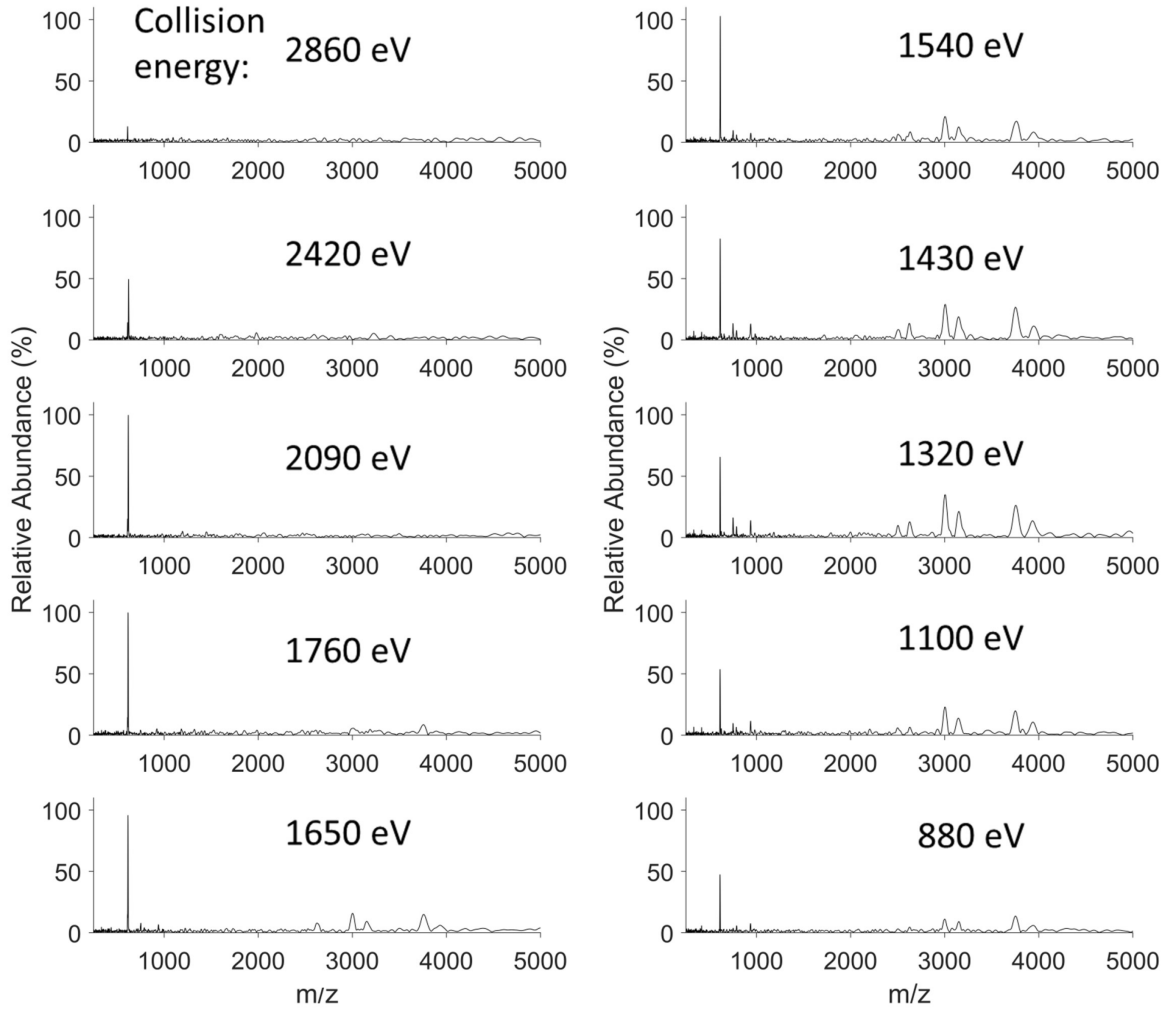

Figure 5: SID product spectra of the 11+ dimer of hemoglobin following isolation, taken at multiple collision energies. The collision energy is controlled by the potential on the SID surface during SID. A post-SID lift to 1980V is used in each case.

3.3 Larger complexes

Two larger protein complexes, creatine phosphokinase and aldolase, were used to demonstrate SID on higher *m/z* species. Creatine phosphokinase is a ~43 kDa protein that exists biologically as a homodimer (86 kDa) in skeletal muscle tissue, located in the cytosol. In the MS1 spectrum in Figure 6, the 16+ and 17+ charge states are observed. Isolation of the 17+ complex was performed as described above. SID shows cleavage of the dimer interface to form monomer with 6+ to 11+ charge states. The distribution is centered around the 8+ and 9+ charge states indicating symmetric charge partitioning, though the monomer charge state distribution observed is broader compared to other proteins, suggesting some unfolding may be taking place. The peak around *m/z* 5000 in the SID spectrum is surviving precursor.

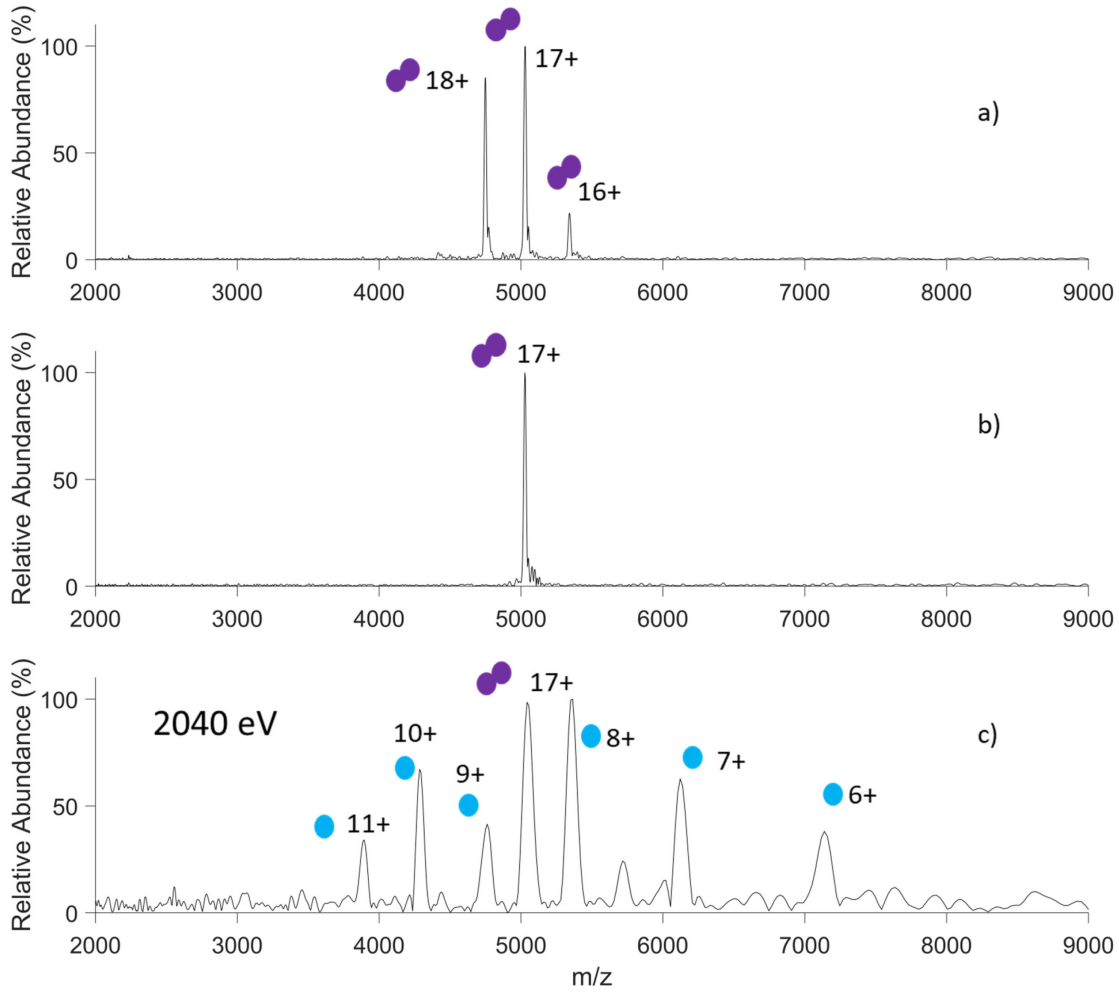

Figure 6: a) MS1 spectrum of creatine phosphokinase, 50 ms transient**.** b) Mirror-switching isolation of the dimer 17+ charge state, 50 ms transient. c) SID spectrum, 4 ms transient.

Aldolase is a 39.2 kDa protein found primarily as a homo-tetramer (156.8 kDa). Figure 7 shows the MS1 spectrum (Figure 7a), spectrum after isolation of the 25+ charge state (Figure 7b), and SID spectrum of the 25+ charge state of aldolase (Figure 7c). Over a range of 500 to 6000 eV, the only observed SID products corresponded to the monomer.

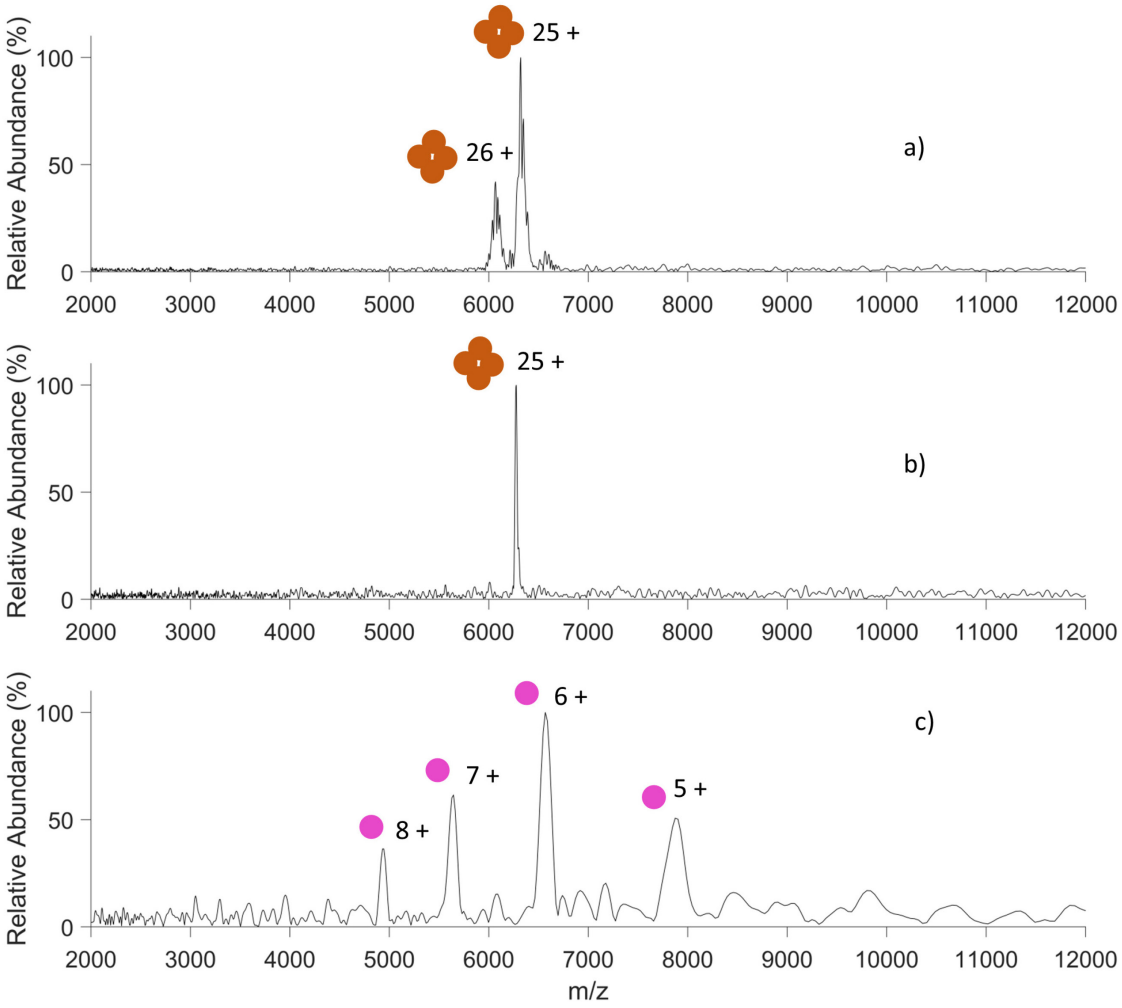

Figure 7: a) MS1 spectrum of aldolase, 50 ms transient**.** b) Mirror-switching isolation of the tetramer 25+ charge state, 50 ms transient. c) 5000 eV SID spectrum, 4 ms transient.

For all of the protein complexes studied here, the signal following SID was much lower than the MS1 signal. Comparing the sum FT peak intensity of SID products to the isolated precursor intensity at the same transient length shows >80% loss of signal following SID. This inefficiency in conversion of signal required the use of shorter transient times for MS2 spectra, thereby resulting in poorer resolution in the MS2 spectra. Various factors likely contribute to this inefficiency, including neutralization and inefficient capture of SID products due to scattered trajectories following SID.

4. Conclusions

The successful implementation of SID as part of a tandem mass spectrometry experiment involving ion isolation, ion dissociation, and product ion mass analysis, on protein complex ions generated under native MS conditions has been demonstrated. While the ELIT mass analyzer has shown good MS1 performance, reaching resolutions over 100,000, and efficient ion isolation has been demonstrated, the ability to perform activation of ions within the mass analyzer has been

limited,[50,51,52,53,54] particularly for high mass ions. While the SID experiment has been demonstrated, the overall efficiency of the process (<20%) is relatively poor using the approach described herein. Furthermore, the trapping efficiency of the product ions is relatively limited such that the collection of frequency data is only possible over short periods of time (e.g., transients of a few ms). These deficiencies currently limit the resolution and sensitivity of the tandem MS experiment using SID. Improvements might be realized by reducing neutralization, perhaps via use of different SID surface modification, and improved detection efficiency in the current system. The latter improvement would enable the collection of longer transients before ion signal drops below the limit of detection. Improvement of the trapping time for the SID product ions is also highly desirable, which would likely require reduction of the angular, and perhaps energy, distributions of products.

Acknowledgments

This work was supported by the National Science Foundation under Grant CHE-170833. This work is dedicated to Professor Vicki Wysocki for the pioneering work that she and her collaborators have performed in the development of SID, particularly with regard to native mass spectrometry. We acknowledge Dr. James W. Hager and Dr. Eric Dziekonski of for helpful discussions, and AB Sciex for providing the QLIT and data analysis software.

References

1 Zajfman, D., Heber, O., Vejby-Christensen, L., Ben-Itzhak, I., Rappaport, M., Fishman, R., Dahan, M. (1997). Electrostatic bottle for long-time storage of fast ion beams. *Physical Review A*, *55*(3), R1577–R1580. https://doi.org/10.1103/PhysRevA.55.R1577

2 Zajfman, D., Rudich, Y., Sagi, I., Strasser, D., Savin, D. W., Goldberg, S., Rappaport, M., Heber, O. (2003). High resolution mass spectrometry using a linear electrostatic ion beam trap. *International Journal of Mass Spectrometry*, *229*(1–2), 55–60. https://doi.org/10.1016/S1387-3806(03)00255-0

3 Dziekonski, E. T., Santini, R. E., McLuckey, S. A. (2016). A dual detector Fourier transform electrostatic linear ion trap utilizing in-trap potential lift. *International Journal of Mass Spectrometry*, *405*, 1–8. https://doi.org/10.1016/j.ijms.2016.05.010

4 Hilger, R. T., Dziekonski, E. T., Santini, R. E., McLuckey, S. A. (2015). Injecting electrospray ions into a Fourier transform electrostatic linear ion trap. *International Journal of Mass Spectrometry*, *378*, 281–287. https://doi.org/10.1016/j.ijms.2014.09.005

5 Pedersen, H. B., Strasser, D., Heber, O., Rappaport, M. L., Zajfman, D. (2002). Stability and loss in an ion-trap resonator. *Physical Review A*, *65*(4), 042703. https://doi.org/10.1103/PhysRevA.65.042703

6 Wollnik, H. (1994). Energy-isochronous time-of-flight mass analyzers. *Int. J. Mass Spectrom. Ion Processes*, 21, 401-403.

7 Pedersen, H. B., Strasser, D., Ring, S., Heber, O., Rappaport, M. L., Rudich, Y., Sagi, I., Zajfman, D. (2001). Ion Motion Synchronization in an Ion-Trap Resonator. *Physical Review Letters*, *87*(5), 055001. https://doi.org/10.1103/PhysRevLett.87.055001

8 Hogan, J. A., Jarrold, M. F. (2018). Optimized Electrostatic Linear Ion Trap for Charge Detection Mass Spectrometry. *Journal of the American Society for Mass Spectrometry*, *29*(10), 2086–2095. https://doi.org/10.1007/s13361-018-2007-x

9 Ring, S., Pedersen, H. B., Heber, O., Rappaport, M. L., Witte, P. D., Bhushan, K. G., Altstein, N., Rudich, Y., Sagi, I., Zajfman, D. (2000). Fourier Transform Time-of-Flight Mass Spectrometry in an Electrostatic Ion Beam Trap. *Analytical Chemistry*, *72*(17), 4041–4046. https://doi.org/10.1021/ac000317h

10 Ayet San Andrés, S., Hornung, C., Ebert, J., Plaß, W. R., Dickel, T., Geissel, H., Scheidenberger, C., Bergmann, J., Greiner, F., Haettner, E., Jesch, C., Lippert, W., Mardor, I., Miskun, I., Patyk, Z., Pietri, S., Pihktelev, A., Purushothaman, S., Reiter, M. P., Rink, A.-K., Weick, H., Yavor, M.I., Bagchi, S., Charviakova, V., Constantin, P., Diwisch, M., Finlay, A., Kaur, S., Knöbel, R., Lang, J.; Mei, B., Moore, I.D., Otto, J.-H., Pohjalainen, Prochazka, A., Rappold, C., Takechi, M., Tanaka, Y.K., Winfield, J.S., Xu, X. (2019). High-resolution, accurate multiple-reflection time-of-flight mass spectrometry for short-lived,

exotic nuclei of a few events in their ground and low-lying isomeric states. *Physical Review C*, *99*(6), 064313. https://doi.org/10.1103/PhysRevC.99.064313

11 Dickel, T., Plaß, W. R., Lang, J., Ebert, J., Geissel, H., Haettner, E., Jesch, C., Lippert, W., Petrick, M., Scheidenberger, C., Yavor, M. I. (2013). Multiple-reflection time-of-flight mass spectrometry for in situ applications. *Nuclear Instruments and Methods in Physics Research Section B: Beam Interactions with Materials and Atoms*, *317*, 779–784. https://doi.org/10.1016/j.nimb.2013.08.021

12 Dziekonski, E. T., Johnson, J. T., Lee, K. W., McLuckey, S. A. (2017). Fourier-Transform MS and Closed-Path Multireflection Time-of-Flight MS Using an Electrostatic Linear Ion Trap. *Analytical Chemistry*, *89*(20), 10965–10972. https://doi.org/10.1021/acs.analchem.7b02797

13 Eliuk, S., Makarov, A. (2015). Evolution of Orbitrap Mass Spectrometry Instrumentation. *Annu. Rev. Anal. Chem. 8*, 61-80.

14 Lössl, P., Snijder, J., Heck, A. J. R. (2014). Boundaries of Mass Resolution in Native Mass Spectrometry. *Journal of the American Society for Mass Spectrometry*, *25*(6), 906–917. https://doi.org/10.1007/s13361-014-0874-3

15 Wargacki, A. J., Wörner, T. P., Van De Waterbeemd, M., Ellis, D., Heck, A. J. R., King, N. P. (2021). Complete and cooperative in vitro assembly of computationally designed self-assembling protein nanomaterials. *Nature Communications*, *12*(1), 883. https://doi.org/10.1038/s41467-021-21251-y

16 Banerjee, S., Mazumdar, S. (2012) Electrospray Ionzation Mass Spectrometry: A Technique to Access the Information Beyond the Molecular Weight of the Analyte. Int. J. Anal. Chem. 2012, 282574.

17 Ganem, B., Li, Y. T., Henion, J. D. (1991). Observation of noncovalent enzyme-substrate and enzyme-product complexes by ion-spray mass spectrometry. *Journal of the American Chemical Society*, *113*(20), 7818–7819. https://doi.org/10.1021/ja00020a085

18 Englander, J. J., Del Mar, C., Li, W., Englander, S. W., Kim, J. S., Stranz, D. D., Hamuro, Y., Woods, V. L. (2003). Protein structure change studied by hydrogen-deuterium exchange, functional labeling, and mass spectrometry. *Proceedings of the National Academy of Sciences*, *100*(12), 7057–7062. https://doi.org/10.1073/pnas.1232301100

19 Tang, X., Munske, G. R., Siems, W. F., Bruce, J. E. (2005). Mass Spectrometry Identifiable Cross-Linking Strategy for Studying Protein−Protein Interactions. *Analytical Chemistry*, *77*(1), 311–318. https://doi.org/10.1021/ac0488762

20 Sinz, A. (2006). Chemical cross-linking and mass spectrometry to map three-dimensional protein structures and protein–protein interactions. *Mass Spectrometry Reviews*, *25*(4), 663–682. https://doi.org/10.1002/mas.20082

21 McLuckey, S. A. (1992). Principles of collisional activation in analytical mass spectrometry. *Journal of the American Society for Mass Spectrometry*, *3*(6), 599–614. https://doi.org/10.1016/1044-0305(92)85001-Z

22 Benesch, J. L. P. (2009). Collisional activation of protein complexes: Picking up the pieces. *Journal of the American Society for Mass Spectrometry*, *20*(3), 341–348. https://doi.org/10.1016/j.jasms.2008.11.014

23 Greisch, J.-F., Tamara, S., Scheltema, R. A., Maxwell, H. W. R., Fagerlund, R. D., Fineran, P. C., Tetter, S., Hilvert, D., & Heck, A. J. R. (2019). Expanding the mass range for UVPD-based native top-down mass spectrometry. *Chemical Science*, *10*(30), 7163–7171. https://doi.org/10.1039/C9SC01857C

24 Zhang, H., Cui, W., Wen, J., Blankenship, R. E., & Gross, M. L. (2011). Native Electrospray and Electron-Capture Dissociation FTICR Mass Spectrometry for Top-Down Studies of Protein Assemblies. *Analytical Chemistry*, *83*(14), 5598–5606. https://doi.org/10.1021/ac200695d

25 Zhang, H., Cui, W., Wen, J., Blankenship, R. E., & Gross, M. L. (2010). Native electrospray and electron-capture dissociation in FTICR mass spectrometry provide top-down sequencing of a protein component in an intact protein assembly. *Journal of the American Society for Mass Spectrometry*, *21*(12), 1966–1968. https://doi.org/10.1016/j.jasms.2010.08.006

26 Zhang, J., Malmirchegini, G. R., Clubb, R. T., & Loo, J. A. (2015). Native Top-down Mass Spectrometry for the Structural Characterization of Human Hemoglobin. *European Journal of Mass Spectrometry*, *21*(3), 221–231. https://doi.org/10.1255/ejms.1340

27 Jones, C. M., Beardsley, R. L., Galhena, A. S., Dagan, S., Cheng, G., Wysocki, V. H. (2006). Symmetrical Gas-Phase Dissociation of Noncovalent Protein Complexes via Surface Collisions. *Journal of the American Chemical Society*, *128*(47), 15044–15045. https://doi.org/10.1021/ja064586m

28 Zhou, M., Dagan, S., Wysocki, V. H. (2012). Protein Subunits Released by Surface Collisions of Noncovalent Complexes: Nativelike Compact Structures Revealed by Ion Mobility Mass Spectrometry. *Angewandte Chemie International Edition*, *51*(18), 4336–4339. https://doi.org/10.1002/anie.201108700

29 Wysocki, V. H., Jones, C. M., Galhena, A. S., Blackwell, A. E. (2008). Surface-induced dissociation shows potential to be more informative than collision-induced dissociation for structural studies of large systems. *Journal of the American Society for Mass Spectrometry*, *19*(7), 903–913. https://doi.org/10.1016/j.jasms.2008.04.026

30 Harvey, S. R., Seffernick, J. T., Quintyn, R. S., Song, Y., Ju, Y., Yan, J., Sahasrabuddhe, A. N., Norris, A., Zhou, M., Behrman, E. J., Lindert, S., Wysocki, V. H. (2019). Relative interfacial cleavage energetics of protein complexes revealed by surface collisions. *Proceedings of the National Academy of Sciences*, *116*(17), 8143–8148. https://doi.org/10.1073/pnas.1817632116

31 Hilger, R.T., Santini, R.E., McLuckey, S.A. (2013) Nondestructive Tandem Mass Spectrometry Using a Linear Quadrupole Ion Trap Coupled to a Linear Electrostatic Ion Trap. *Anal. Chem.*, *85*, 5226-5232.

32 Johnson, J.T., Lee, K.W., Bhanot, J.S., McLuckey, S.A. (2019) A Miniaturized Fourier Transform Electrostatic Linear Ion Trap Mass Spectrometer: Mass Range and Resolution. *J. Am. Soc. Mass Spectrom.*, *30*, 588-594. DOI 10.1007/s13361-018-02126-x

33 Dziekonski, E.T., Johnson, J.T., Lee, K.W., McLuckey, S.A. (2017) Fourier-transform MS and Closed-path Multi-reflection Time-of-Flight MS using an Electrostatic Linear Ion Trap. *Anal. Chem.*, *89*, 10965-10972.

34 Hilger, R.T., Santini, R.E., McLuckey, S.A. (2014) Square Wave Modulation of a Mirror Lens for Ion Isolation in a Fourier Transform Electrostatic Linear Ion Trap Mass Spectrometer. *Int. J. Mass Spectrom.*, *362*, 1-8.

35 Johnson, J.T., Eakins, G.S., McLuckey, S.A. (2019) Mirror Switching for High Resolution Ion Isolation in an Electrostatic Linear Ion Trap. *Anal. Chem.*, *91*, 8789-8794.

36 Johnson, J.T., Carrick, I.J., Eakins, G.S., McLuckey, S.A. (2019) Simultaneous Isolation of Non-Adjacent *m/z* Ions Using Mirror Switching in an Electrostatic Linear Ion Trap. *Anal. Chem*., *91*, 12574-12580.

37 Fischer, P., Schweikhard, L. (2019) Photofragmentation of $Bi_n^{+/-}$ clusters (n=2-19) in an electrostatic ion beam trap. Eur. Phys. J. D, 73, 105. https://doi.org/10.1140/epjd/e2019-100027-0

38 Hilger, R.T., Santini, R.E., McLuckey, S.A. (2014) Tandem Mass Spectrometry in an Electrostatic Linear Ion Trap Modified for Surface-induced Dissociation. Anal. Chem., 86 (2014) 8822-8828.

39 Hogan, J. A., Jarrold, M. F. (2018). Optimized Electrostatic Linear Ion Trap for Charge Detection Mass Spectrometry. *Journal of The American Society for Mass Spectrometry*, *29*(10), 2086–2095. https://doi.org/10.1007/s13361-018-2007-x

40 Thomson, B.A.; Jolliffe, C.L.; U.S. Patent, 5,847,386.

41 Loboda, A.; Krutchinsky, A.; Loboda, O.; McNabb, J.; Spicer, V.; Ens, W.; Standing, K. (2000) Novel LINAC II electrode geometry for creating an axial field in a multipole ion guide. *Eur. J. Mass Spectrom.*, *6*, 531-536.

42 Lange, O.; Damoc, E.; Wieghaus, A.; Makarov, A. (2014) Enhanced Fourier transform for Orbitrap mass spectrometry. *International Journal of Mass Spectrometry*, 369, 16-22.

43 Hilger, R.T.; Wyss, P.J.; Santini, R.E.; McLuckey, S.A. (2013) Absorption Mode Fourier Transform Electrostatic Linear Ion Trap Mass Spectrometry. Analytical Chemistry, 85, 8075-8079.

44 Johnson, J. T., Carrick, I. J., Eakins, G. S., McLuckey, S. A. (2019). Mirror Switching for High-Resolution Ion Isolation in an Electrostatic Linear Ion Trap. *Analytical Chemistry*, *91*(14), 8789–8794. https://doi.org/10.1021/acs.analchem.9b00874

45 Jones, C. M., Beardsley, R. L., Galhena, A. S., Dagan, S., Cheng, G., Wysocki, V. H. (2006). Symmetrical Gas-Phase Dissociation of Noncovalent Protein Complexes via Surface Collisions. *Journal of the American Chemical Society*, *128*(47), 15044–15045. https://doi.org/10.1021/ja064586m

46 Snyder, D. T., Lin, Y.-F., Somogyi, A., Wysocki, V. H. (2021). Tandem surface-induced dissociation of protein complexes on an ultrahigh resolution platform. *International Journal of Mass Spectrometry*, *461*, 116503. https://doi.org/10.1016/j.ijms.2020.116503

47 Wang, J., Meroueh, S. O., Wang, Y., Hase, W. L. (2003). Efficiency of energy transfer in protonated diglycine and dialanine SID. *International Journal of Mass Spectrometry*, *230*(1), 57–63. https://doi.org/10.1016/j.ijms.2003.08.005

48 Schultz, D. G., Lim, H., Garbis, S., Hanley, L. (1999). Energy partitioning in the surface-induced dissociation of linear and cyclic protonated peptides at an organic surface. *Journal of Mass Spectrometry*, *34*(3), 217–225. https://doi.org/10.1002/(SICI)1096-9888(199903)34:3<217::AID-JMS797>3.0.CO;2-R

49 De Clercq, H. L., Sen, A. D., Shukla, A. K., Futrell, J. H. (2001). Inelastic ion-surface collisions: Scattering and dissociation of low energy benzene molecular cations. *International Journal of Mass Spectrometry*, *212*(1–3), 491–504. https://doi.org/10.1016/S1387-3806(01)00509-7

50 Ayet San Andrés, S., Hornung, C., Ebert, J., Plaß, W. R., Dickel, T., Geissel, H., Scheidenberger, C., Bergmann, J., Greiner, F., Haettner, E., Jesch, C., Lippert, W., Mardor, I., Miskun, I., Patyk, Z., Pietri, S., Pihktelev, A., Purushothaman, S., Reiter, M. P., Rink, A.-K., Weick, H., Yavor, M.I., Bagchi, S., Charviakova, V., Constantin, P., Diwisch, M., Finlay, A., Kaur, S., Knöbel, R., Lang, J.; Mei, B., Moore, I.D., Otto, J.-H., Pohjalainen, Prochazka, A., Rappold, C., Takechi, M., Tanaka, Y.K., Winfield, J.S., Xu, X. (2019). High-resolution, accurate multiple-reflection time-of-flight mass spectrometry for short-lived, exotic nuclei of a few events in their ground and low-lying isomeric states. *Physical Review C*, *99*(6), 064313. https://doi.org/10.1103/PhysRevC.99.064313

51 Doussineau, T., Antoine, R., Santacreu, M., Dugourd, P. (2012). Pushing the Limit of Infrared Multiphoton Dissociation to Megadalton-Size DNA Ions. *The Journal of Physical Chemistry Letters*, *3*(16), 2141–2145. https://doi.org/10.1021/jz300844e

52 Doussineau, T., Yu Bao, C., Clavier, C., Dagany, X., Kerleroux, M., Antoine, R., Dugourd, P. (2011). Infrared multiphoton dissociation tandem charge detection-mass spectrometry of single megadalton electrosprayed ions. *Review of Scientific Instruments*, *82*(8), 084104. https://doi.org/10.1063/1.3628667

53 Fischer, P., Schweikhard, L. (2019). Photofragmentation of Bin+/- clusters (n = 2−19) in an electrostatic ion beam trap. *The European Physical Journal D*, *73*(5), 105. https://doi.org/10.1140/epjd/e2019-100027-0

54 Antoine, R., Doussineau, T., Dugourd, P., Calvo, F. (2013). Multiphoton dissociation of macromolecular ions at the single-molecule level. *Physical Review A*, *87*(1), 013435. https://doi.org/10.1103/PhysRevA.87.013435